

Supercapacitor Nanofiber Electrodes Graphene-Based

Mustafa H. Mustafa*, Alan Zdunek*

University of Illinois at Chicago, Department of Mechanical, Chemical Engineering (MC 110), 842 West Taylor Street, Chicago, IL 60607-7022

*Email: mmusta4@gmail.com, zdunek@uic.edu

Received: 5 September 2016 / Accepted: 6 January 2017 / Published: 12 March 2017

Carbon-based polyacrylonitrile (PAN) nanofiber mats formed via the electrospinning process with varying amounts of graphene and carbon black were used as electrodes in single cell supercapacitor experiments in 1M H₂SO₄. A strong influence of initial electrospinning mixture concentration on capacitance and electrode structure was observed. Electrodes fabricated from a lower carbon mixture containing PAN and graphene showed the highest capacitances whereas electrodes fabricated from higher carbon mixtures of PAN, graphene and carbon black had significantly lower capacitance values. Transmission electron microscope (TEM) images show an amorphous carbon structure for electrodes with the highest capacitance value whereas a turbostratic structure was more prevalent for the lower capacitance supercapacitors.

Keywords: Supercapacitor; Nanofiber; Electrode; Graphene; Electrospinning

1. INTRODUCTION

Carbon-based supercapacitors are promising next generation energy storage devices due to their high surface area, non-toxicity, chemical stability, abundance, and low cost [1,2]. Currently, several methods are used to manufacture supercapacitors, including screen printing [3,4], coating [5] and spray technology [6]. However, some of these methods require a binder, like polytetrafluoroethylene (PTFE), to keep the carbon particles compacted for capacitance storage. Without the binder, carbon particles will migrate and disperse, causing gaps and high resistivity that reduce the efficiency and performance of energy storage. Furthermore, the binder adds another step in the manufacturing process, which induces additional cost.

A novel approach that eliminates the binding operation, improves the compaction of carbon particles and increases the conductivity of the electrode material is the electrospinning process. Electrospinning is a well-known technique used to produce polymer nanofibers for nanocomposite

applications [7,8]. Carbon nanofibers have previously been manufactured by electro-spinning on conductive substrates to create a fiber mat electrode for energy storage [9,10]. Electrospinning uses a conductive solution that is subjected to a high voltage potential (~12kV) to create web-like nanofiber strings that are collected on a substrate to create mats for electrodes, as seen in Figure 1. Nanofiber mats manufactured using a polyacrylonitrile (PAN) solution exhibit good electrical conductivity for use as electrodes [8,11]. In addition, the PAN solution can be mixed with additional carbon-based materials such as graphene or carbon black to further increase the electrical conductivity in the homogenous mixture and ultimately create nanofiber mats with better electrode characteristics [9]. Graphene is a thin layer of carbon one atom thick with a crystalline structure that is electrically conductive. It improves the overall conductivity of the polyacrylonitrile (PAN) fibers by creating carbon sheets with a uniform structure that is thought to enhance the flow of electrons, allowing additional paths for electrons to travel through the nanofiber mats. Carbon Black (CB) is an amorphous structure of carbon that is also referred to as free carbon, without a crystalline structure. Carbon black can also be used to enhance overall conductivity of the electrospun fibers. Subsequently, the electrospinning method avoids the need for the secondary binding process in the traditional supercapacitor electrode manufacturing method. Although this creates an advantage over traditional methods, the electrospinning process is governed by the conductivity of the solution and the amount of added carbon-based material, causing limitations on industrial scale usage by limiting the type of materials that can be fabricated. Also, the free standing nanofiber webs are brittle and require careful handling [1]. Furthermore, electrospinning can have high sample to sample variation due to the random nature of collecting the nanofibers to create electrode mats. Hence, better process control and optimal manufacturing parameters for the electrospinning process are needed, such as further research to better understand the effects of the electric field strength and stagnation plan on jet path [16], employing a near-field electrospinning process (NFES) [7] or The Tip-Induced Electrospinning process [13].

Research on electrospun activated carbon nanofibers used as electrodes for supercapacitors have concluded that the highest capacitance values correspond to an optimum carbon activation temperature of 800°C, which also corresponded to the largest specific surface area. The research points to a strong dependency of charge resistance and surface area on the performance of supercapacitors [9]. Other research has mainly focused on characterizing the pore size, surface area and resistivity of the nanofiber mats. It was shown that pore size and surface area distribution can improve capacitance, but are not a major factor in increasing capacitance significantly [14,15]. On the other hand, an anomalous increase in carbon capacitance for pore sizes less than 1nm using carbide-derived carbons (CDCs) has been reported in the literature [16]. Additional study on the relationship between ion size and pore size was conducted by Largeot et al. [17] and polarization induced ion distortion in the pores of carbon was reported by Ania et al. [18]. Furthermore, a pseudo-faradaic charge transfer type behavior in the porous regions has been reported by Frackowiak et al. [19].

This research will investigate using various graphene and carbon black concentrations to create nanofiber mats by the electrospinning process and the effect on capacitance and electrode structure for supercapacitors. Carbonized polyacrylonitrile (PAN) nanofiber electrodes with and without carbon black and with varying graphene concentrations will be manufactured by the electrospinning process.

A secondary physical or chemical activation process will not be used to reduce variability in tested samples. Nanofiber material characteristics will be characterized by an element spectral analysis, using an energy dispersive X-ray (EDX) spectroscopy, which measures the emitted peak energy to determine the emissions spectrum of the sample tested; And a transmission electron microscope (TEM) to determine the carbon structure.

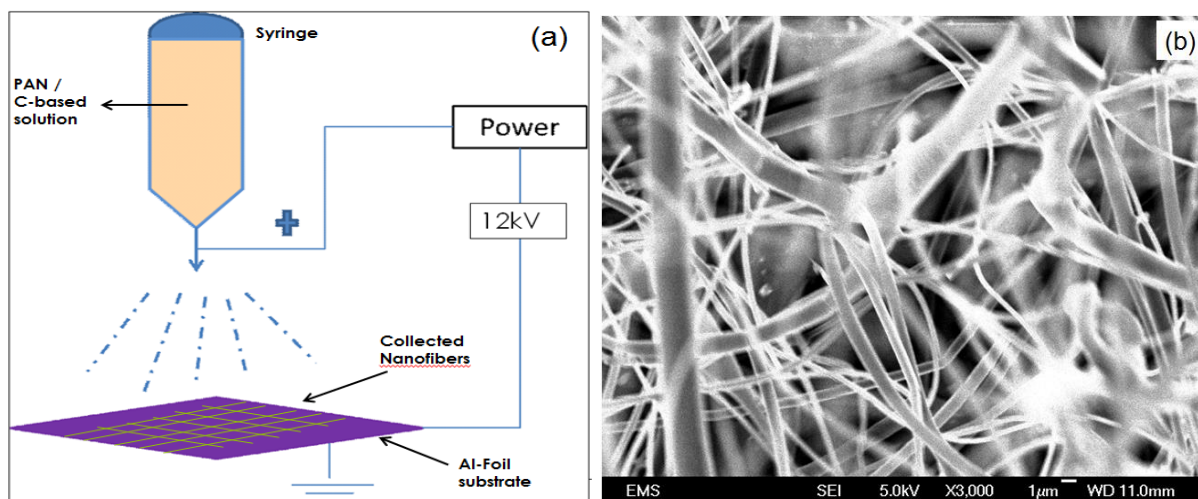


Figure 1. a) Electrospinning process illustration, b) Scanning Electron Microscope (SEM) of collected nanofiber mats

2. EXPERIMENTAL

2.1 Sample Preparation

Carbon nanofiber electrode samples were prepared using the electrospinning process with solution of 8% by wt. PAN-Polyacrylonitrile (MW 150,000) in 100% DMF-N-N dimethylformamide (solvent) and with a 15%, 25% and 35% by weight of graphene oxide (N006-010-P) from Angstrom Materials added to the 8% by wt. PAN. Additional samples were made by adding 10% by wt. carbon black (CB) from Cabot to the 8% by wt. PAN mixture with the same graphene concentrations.

The electrospinning process was used to create the nanofiber mat electrodes. A brief description of the process is given below; additional information on the process and techniques has been defined in the literature [8,20].

The PAN, DMF and additional carbon sources (graphene oxide, carbon black) were placed in a 20ml standard glass container and placed on a heated rotator for 12 hours to stir the mixture and create a homogenous solution. The solution was loaded into a 10cc 18GA needle syringe and allowed to flow at a rate of approximately 1.0mL/hr at a voltage potential of 12.5kV and at a separation distance of 16cm from the aluminum foil collector. The nanofibers were collected on the aluminum foil, creating the nanofiber mats. The samples were then heat treated to 800°C by first ramping up the temperature at a rate of 5° C/min from room temperature to 350°C. A flow of nitrogen at 5ccm was then introduced and the samples were heated from 350°C to 800°C at a rate of 7°C/min. The samples were then cooled

back down to room temperature. The heat treatment of the nanofiber mats carbonizes the (PAN) at elevated temperatures with an inert atmosphere, which removes non-carbon elements. Carbon activation refers to the process of forming pores and pockets in carbon to increase its surface area. Carbon activation is done by physical means such as a suitable oxidizing gas agent (O_2 , CO_2 or steam), or by chemical activation such as (KOH , H_3PO_4 , $ZnCl_2$), followed by carbonization at 400° to $900^\circ C$ [21]. Carbon activation was not performed on the samples to reduce variability and focus on the graphene and carbon black effects on supercapacitance.

Two-electrode supercapacitor test cells were assembled by using two nanofiber mats and separated by an insulator (Cellgard membrane 3501) as shown in Figure 2. The opposite ends of the nanofiber mat samples were in contact with a nickel wire mesh used as a current collector. The two-electrode assembly was clamped with a spring loaded plastic clip (providing an analogy of bolt stretch, used in a conventional supercapacitor). A cotton pad was placed on each end of the nickel wire mesh and wetted with $1M H_2SO_4$. The average area of the nanofiber mat was approximately $0.35 cm^2$ and the depth varied from 0.15-1.10mm thickness. A total of five (5) test cells for each electrode composition were constructed.

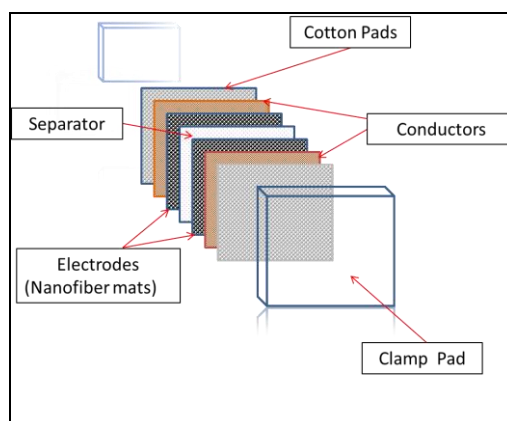


Figure 2. Single-cell Two-electrode assembly with nanofiber mats

2.2 Cyclic Voltammetry (CV)

Supercapacitor test cell performance was measured electrochemically by cyclic voltammetry (CV). The two-electrode test cell was subjected to a voltage range of 0-0.9V and six scan rates between 10-500 mV/s. The scans were performed using a Princeton Applied Research PARSTAT 2273 Advanced Electrochemical System (Potentiostat/Galvanostat) controlled with Power Suite software. In order to perform the scans as a two-electrode system, the counter and reference wires of the instrument were connected to one side of the supercapacitor nanofiber electrode assembly, while the working electrode connection was connected to the other electrode. The linear portion of the (CV) discharge curve, in the range of 0.45 to 0.54V, as shown in dash lines in Figure 3, was used to calculate the specific capacitance at a scan rate of 10mV/s. Figure 3 shows a representative cyclic voltammetric scan for the single-cell test assembly.

The capacitance is defined as:

$$C = Q / V \tag{1}$$

Where C is the capacitance in Farads (F), Q is the charge in coulombs (i.e., the area under the cyclic voltammetry curve), and V is the voltage (V). The charge, Q can also be defined as:

$$Q = \int [I (dt)] \tag{2}$$

Where I is the current in amperes, dt is the discharge time (ms) taken from a linear slope, in the range of 0.45-0.54V .

Therefore, the capacitance becomes:

$$C = \int I \frac{dt}{dV} = Q / dV \tag{3}$$

Where dV is the potential variation in the time range, dt

The specific capacitance (F/g) is calculated by:

$$C_m = C / m \tag{4}$$

Where C_m is the specific capacitance in Farads per gram of the sample (F/g) and m is the weight in grams (g)

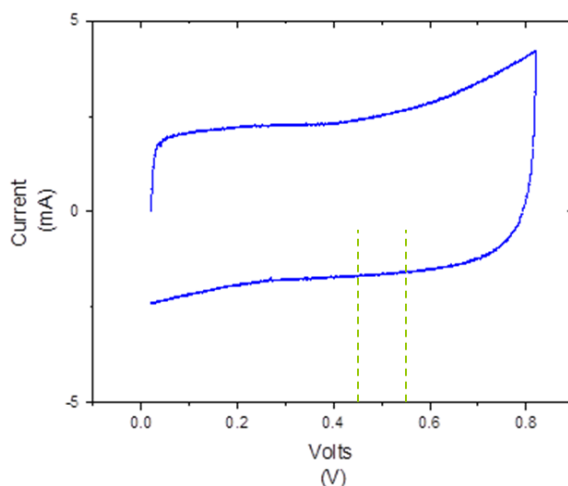


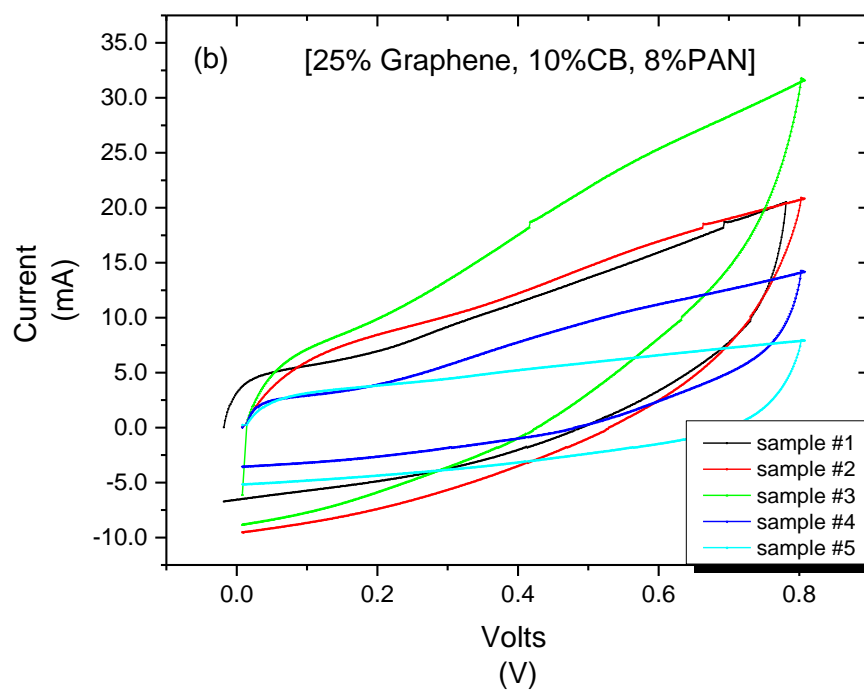
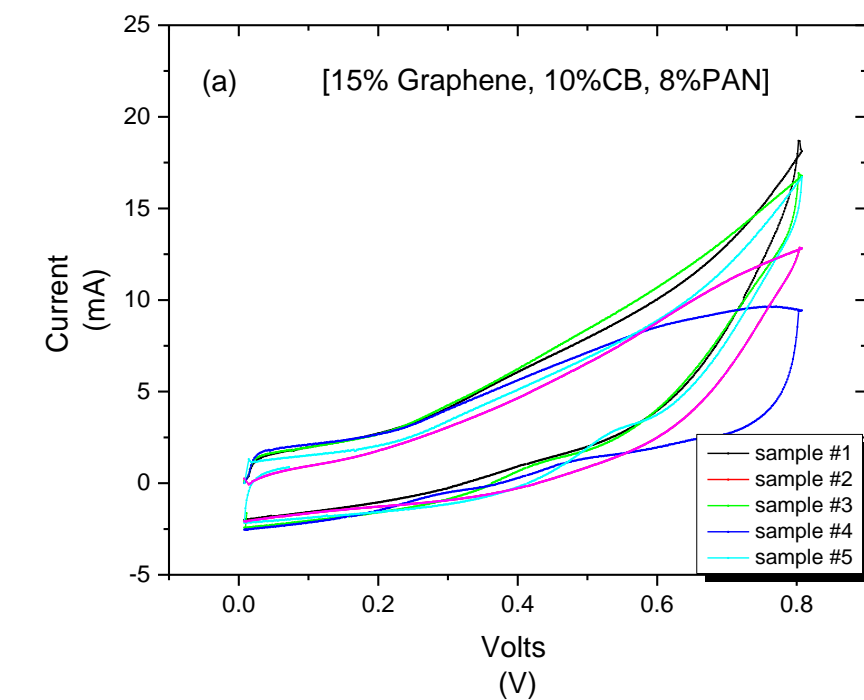
Figure 3. Cyclic Voltammetry (CV) graph showing a typical charge measuring sample location; the specific capacitance is calculated from the linear portion of the discharge curve, which is usually (0.45 to 0.54) volts. The graph above was taken from a carbon based nanofiber mat; 35% graphene, 10% (CB) with 8% PAN at a 10 (mV/s) scan rate.

2.2 Spectrum and Image Analysis

A Hitachi Ltd (S-3000N), Energy Dispersive X-ray (EDX) spectroscopy from Oxford was employed to measure chemical composition of the nanofiber samples. Image analysis of carbon nanofibers were performed with a JEOL JEM-3010 with Gatan digital cameras and Thermo-Noran XEDS transmission electron microscope (TEM).

3. RESULTS AND DISCUSSION

3.1 Cyclic Voltammetry (CV) Results



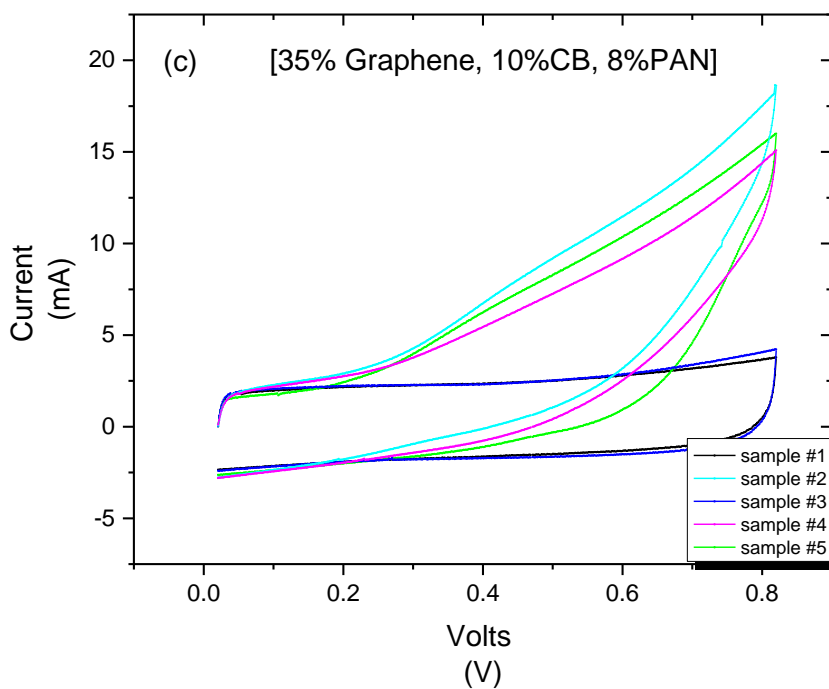
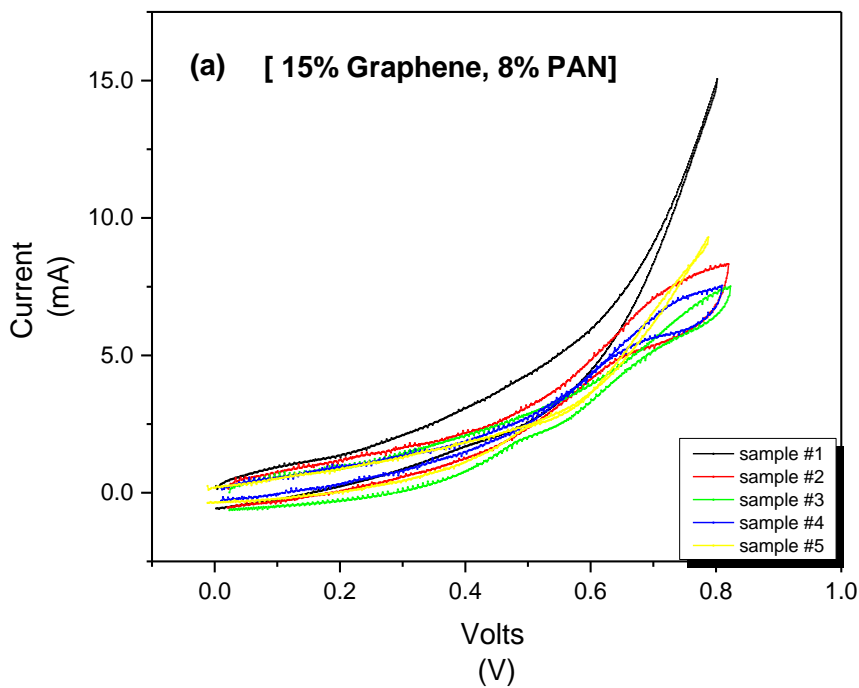
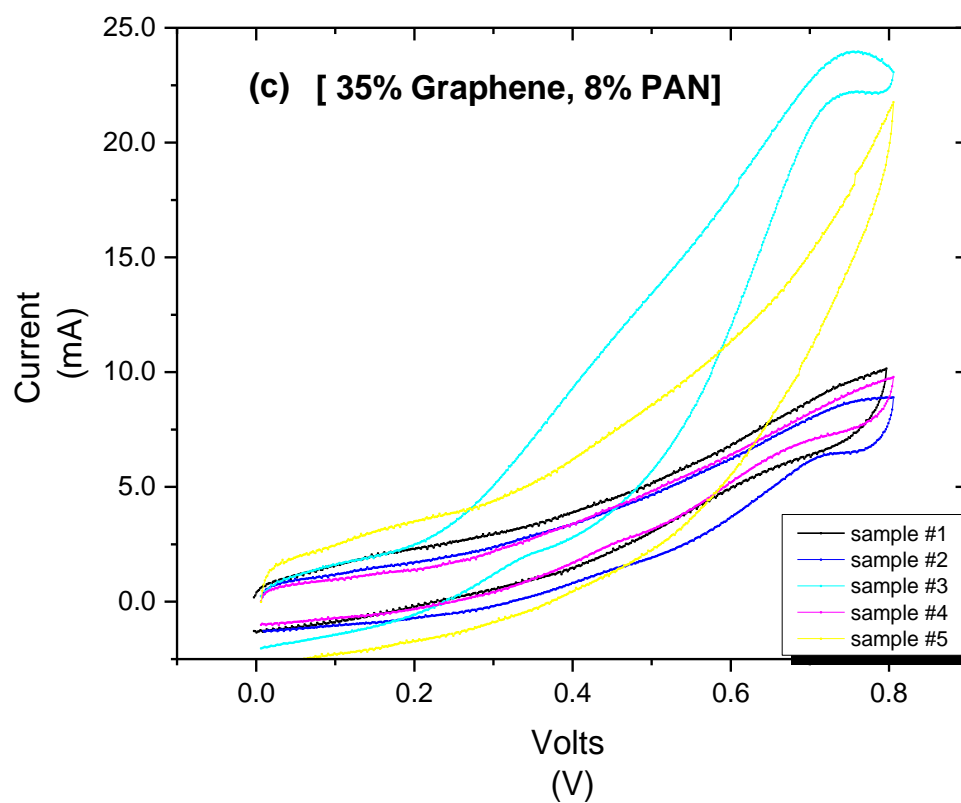
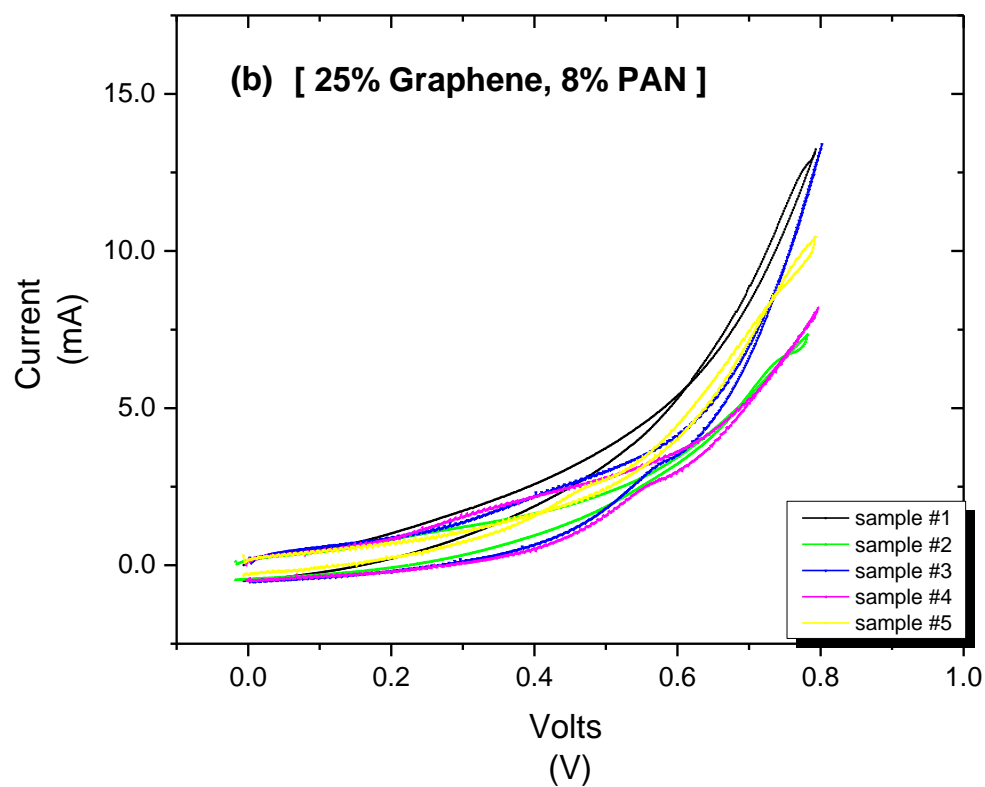


Figure 4. (a) CV graphs for 15% graphene, 10% CB, 8% PAN, heat treated at 800°C, submerged in 1M H₂SO₄ (b) CV graphs for 25% graphene, 10% CB, 8% PAN, heat treated at 800°C, submerged in 1M H₂SO₄ (c) CV graphs for 35% graphene, 10% CB, 8% PAN, heat treated at 800°C, submerged in 1M H₂SO₄





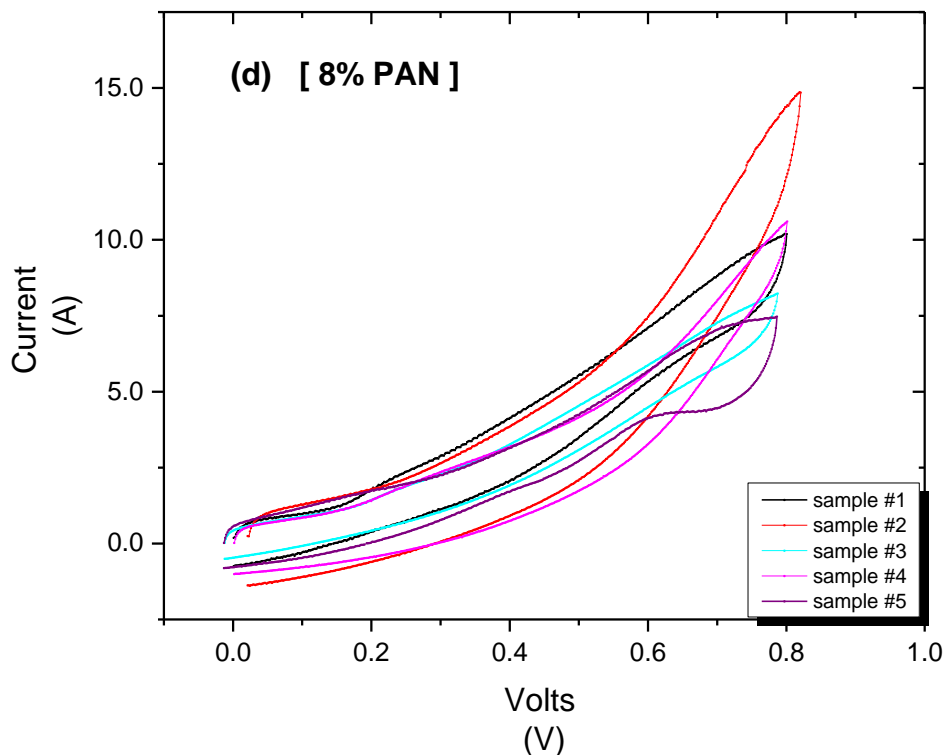


Figure 5. (a) CV graphs for 15% graphene, 8% PAN, heat treated at 800°C, submerged in 1M H₂SO₄. (b) CV graphs for 25% graphene, 8% PAN, heat treated at 800°C, submerged in 1M H₂SO₄. (c) CV graphs for 35% graphene, 8% PAN, heat treated at 800°C, submerged in 1M H₂SO₄. (d) CV graphs for 8% PAN only, heat treated at 800°C, submerged in 1M H₂SO₄.

Figure 4 and Figure 5 show representative (CV) scans for the supercapacitor test cells containing nanofiber electrodes with 8% PAN, 15%, 25% and 35% graphene and with/without 10% carbon black. A sample with only 8% PAN was also tested as shown in Figure 5(d). A total of 5 separate tests were performed for each electrode; the capacitance values are shown in Figure 6.

The specific capacitance calculated from the scans is shown in Figure 6. The 15% & 25% graphene with 8% PAN and the 8% PAN-only samples showed the highest capacitance with average values of 374, 387 and 428 F/g respectively. However, there was a large variation between samples with a maximum capacitance value greater than 600 F/g but with minimum values not lower than 200 F/g. The highest capacitance value of 629 F/g was obtained from the 25% graphene with 8% PAN. The sample variation in capacitance for the 35% graphene with 8% PAN was less, but the total capacitance decreased significantly with an average value of 175 F/g (maximum of 275 F/g and a minimum of 81 F/g). On the other hand, the capacitance values of the 15%, 25% & 35% graphene with 10% (CB) and 8% PAN samples showed much lower sample to sample variation, but gave the lowest capacitance values that predominantly remained under 200 F/g, with the highest being 184 F/g Figure 6.

The electrospinning manufacturing process of collecting the nanofiber mats on an aluminum foil and the variation in solution jetstream during solidification from the high voltage potential can have an effect on sample to sample variation. However, since the same process and voltage were used

for the samples with and without carbon black, sample variation should be similar. The capacitance results show that there is a clear difference in sample to sample variation between the samples with and without carbon black, and that the initial carbon content of the electrospinning solution is influencing the sample variation. The number of moles of carbon for the 15%, 25% & 35% with 10% (CB) and 8% PAN samples were three times greater than the 8% PAN only samples and the samples with 15%, 25% & 35% graphene with 8% PAN, as shown in Table 1 and Figure 7. From the samples tested the higher carbon content corresponded to a lower variation in capacitance Figure 6. However, the higher carbon content mixture produced a lower capacitance. Therefore, optimizing the carbon content is important to reduce sample to sample variation in capacitance and maintain a high capacitance value.

Table 1. Moles of Carbon per 100g solution

Solution (sol.)	Moles Carbon per 100g sol.
8% PAN Only	0.380
15% Grf, 8% PAN	0.386
25% Grf, 8% PAN	0.391
35% Grf, 8% PAN	0.395
15% Grf, 10% C.B, %8 PAN	1.220
25% Grf, 10% C.B, %8 PAN	1.224
35% Grf, 10% C.B, %8 PAN	1.229

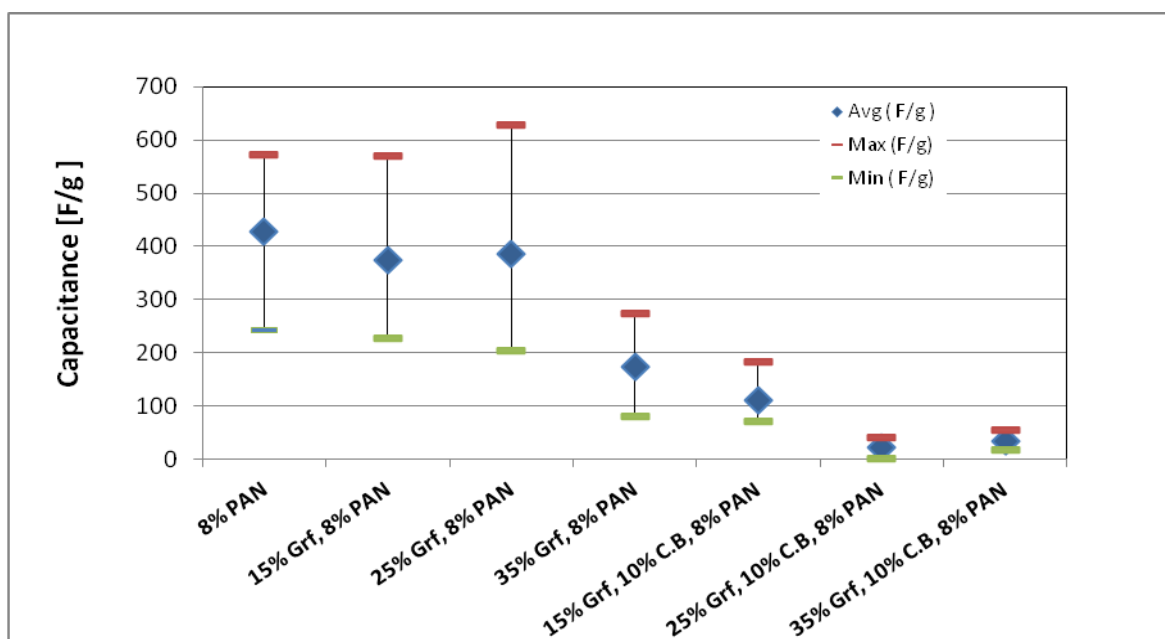


Figure 6. Specific capacitance (F/g) values of various nanofiber mat electrodes

3.2 Spectrum and Image Analysis

A Hitachi Ltd (S-3000N), Energy Dispersive X-ray (EDX) spectroscopy from Oxford Instruments was employed to measure the chemical composition of several selected samples; the 15% and 25% graphene with 10% (CB) and 8% PAN; the 15% graphene with 8% PAN; and the 8% PAN only samples. The spectrum analysis of the samples tested indicates that the main composition of the tested samples is carbon and nitrogen, with smaller traces of oxygen Figure 8.

The carbon to nitrogen (C/N) ratio for the samples are shown in Figure 9; The data is showing a (C/N) atomic ratio in the range of 8 to19 with a spread of less than 5 (C/N) for the samples with the highest capacitance values above 550 F/g; the 15% graphene with 8% PAN and the 8% PAN only samples. An atomic ratio of 4 to 22 (C/N) is seen for the ~ 200 (F/g) sample of 15% graphene, 10% (CB) and 8% PAN. The sample with the lowest capacitance value; 25% graphene, 10% (CB) and 8% PAN showed a wide spread of 12 to 63 C/N atomic ratio as shown in Figure 9. Although the data is showing a lower (C/N) ratio spread for the highest capacitance samples Figure 9, the data is not sufficient to indicate a trend or conclusion.

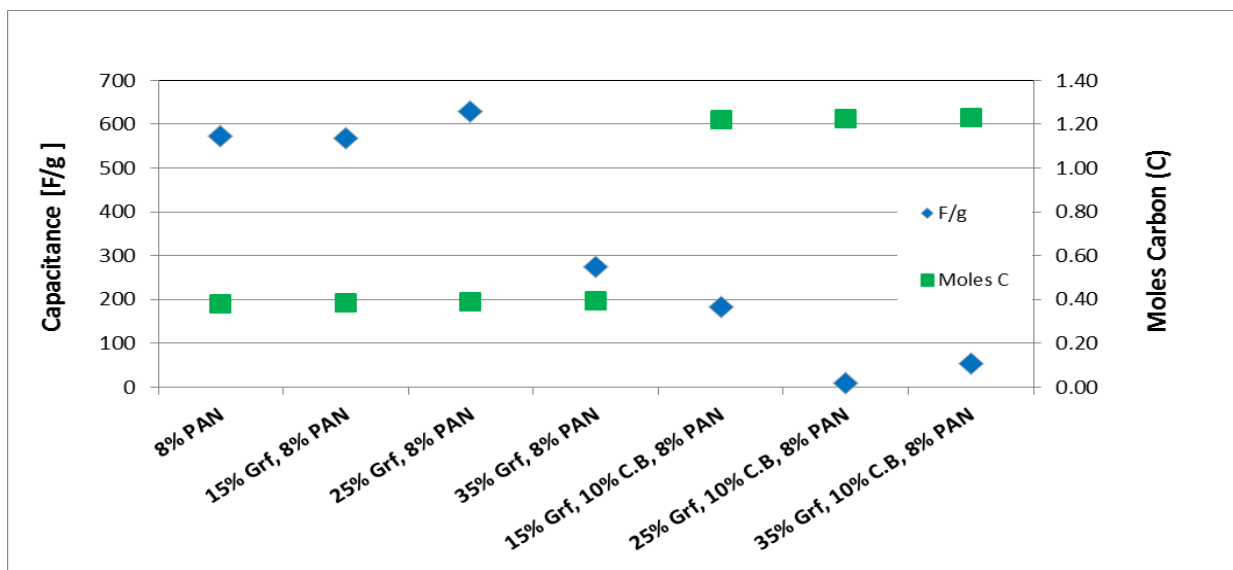
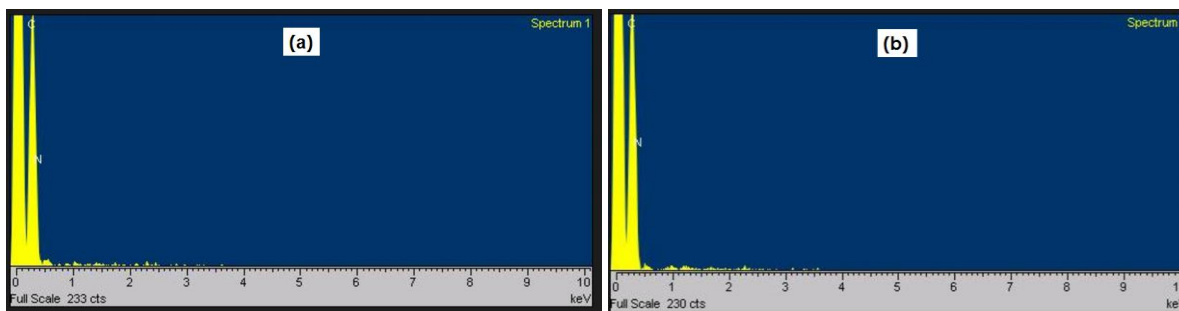


Figure 7. Initial Solution Moles of Carbon vs. Capacitance (F/g)



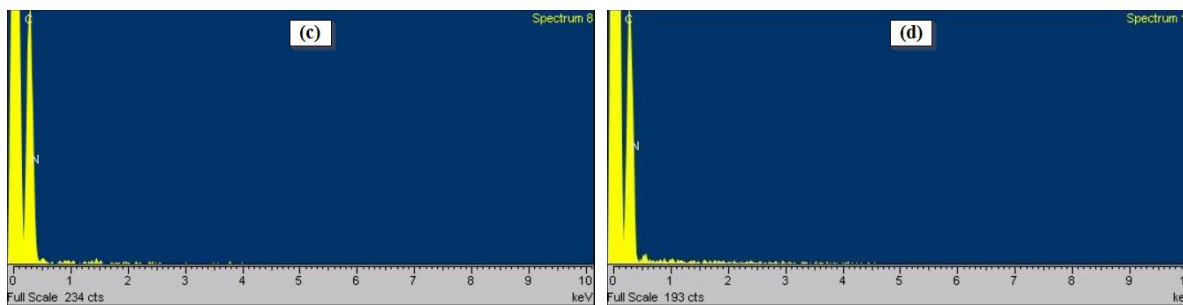


Figure 8. Energy Dispersive X-ray (EDX) Spectrum analysis (a) 15% Graphene, 10% (CB) with 8% PAN; (b) 25% Graphene, 10% (CB) with 8% PAN (c) 15% Graphene with 8% PAN; (d) 8% PAN only

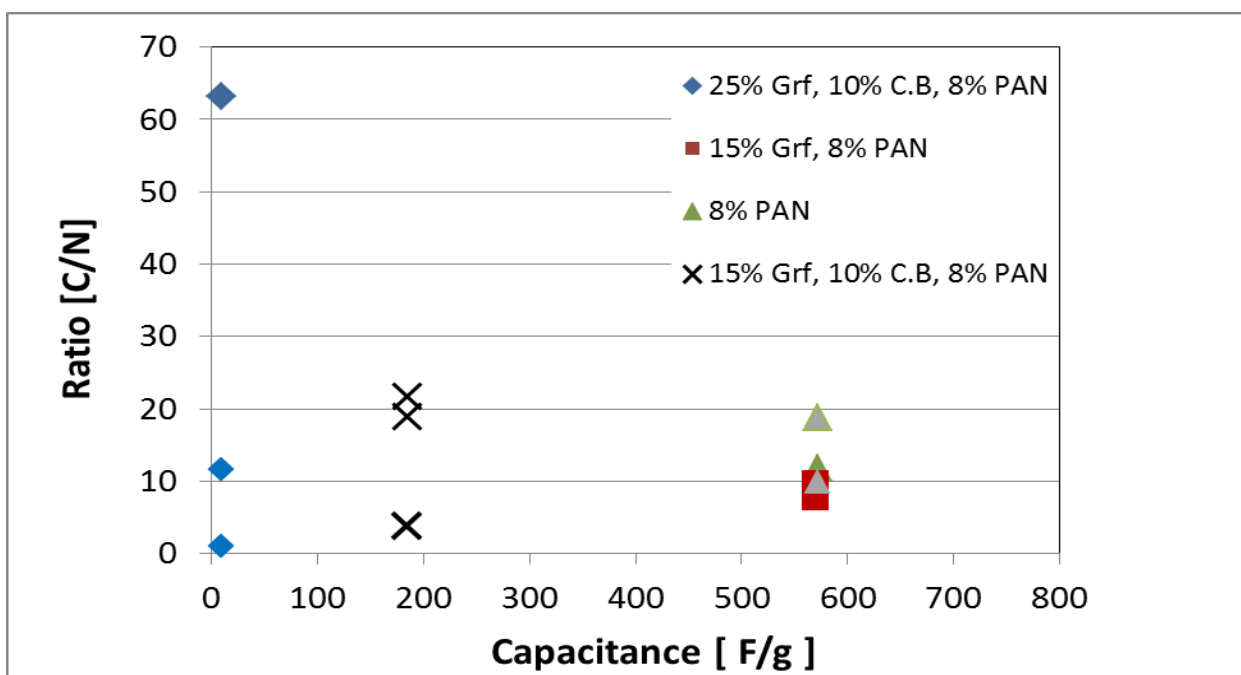


Figure 9. Atomic ratio of Carbon to Nitrogen (C/N) vs. Capacitance (F/g) of Nanofiber mat electrodes

Transmission electron microscope images were made with a JEOL JEM-3010 transmission electron microscope (TEM) with Gatan digital cameras and Thermo-Noran XEDS were analyzed. Two samples were imaged; a high capacitance sample; 15% graphene with 8% PAN, and a lower capacitance sample; 15% graphene, 10% (CB) and 8% PAN. The TEM images are shown in Figure 10 and Figure 11.

The image analysis of the high capacitance 15% graphene with 8% PAN sample suggests that the nanofibers are mainly an amorphous carbon structure. An amorphous structure provides an efficient absorption and release of energy during charging and discharging. This is not fully understood and additional research is needed, however it is believed the amorphous structure has increased vacancies that provide increased energy storage capacity, furthermore the vacancies may allow efficient movement of ions into and out of the structure to further reduce losses. This can be analogous to ion vacancies in perovskite materials in solid 0D nanostructures or oxygen vacancies in 1D Nanorods [22].

There does not seem to be a correlation between nanofiber mat electrode thickness and capacitance with the tested samples Figure 12.

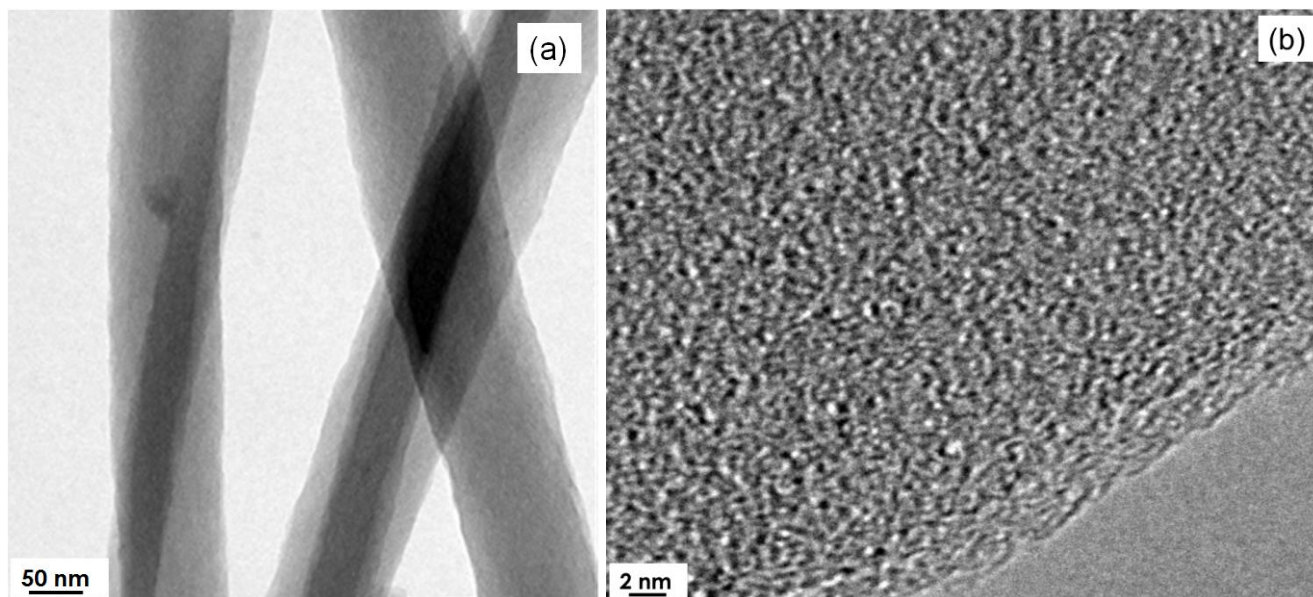


Figure 10. (a) Transmission Electron Microscope (TEM) analysis of 15% graphene with 8% PAN nanofiber electrode (b) TEM magnification shows an amorphous carbon (without a crystalline structure), also known as free, reactive carbon and is referred to as allotrope of carbon.

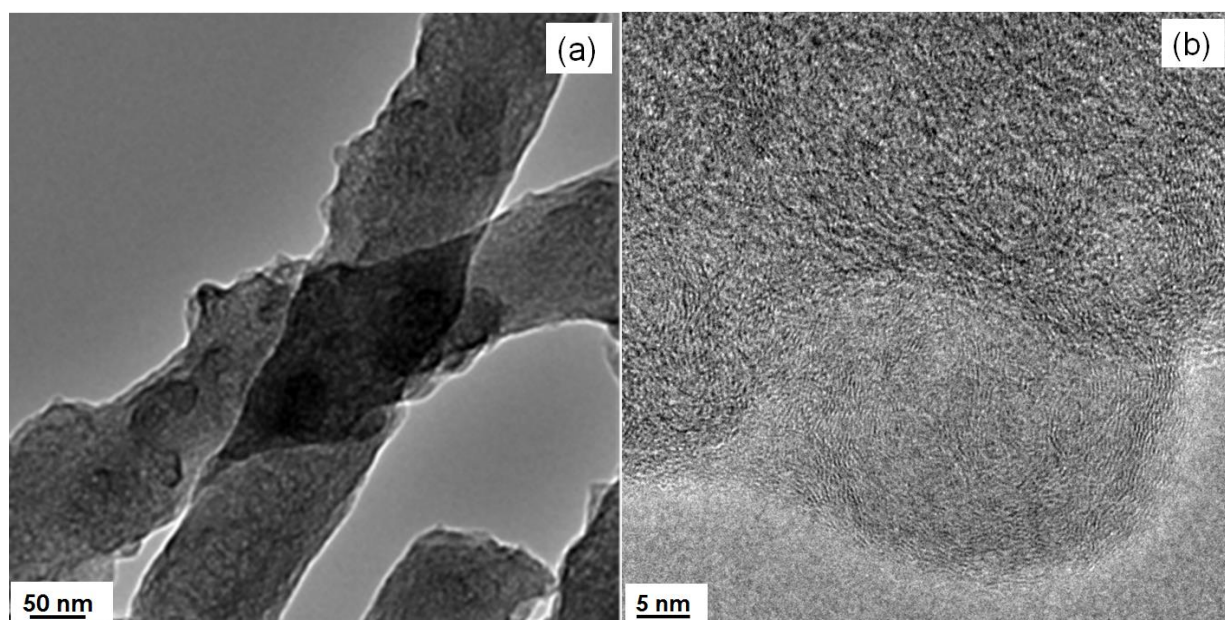


Figure 11. (a) Transmission Electron Microscope (TEM) analysis of 15% graphene, 10% (CB) and 8% PAN nanofiber electrode (b) TEM magnification shows a turbostratic crystallite structure, which is defined as a porous intermediate stage between amorphous carbon and graphene sheet

This is contrary to reported literature regarding the limitation of ion diffusion with increased electrode thickness [23,24]. This can be explained by the thicknesses used in the reported literature,

which is an order of magnitude higher than the samples used in this experiment. Another explanation is the way the nanofiber mat composition was created with the electrospinning process, which deposits nanofiber mats on top of each other, creating a highly porous structure that allows minimal restrictions to ion flow. The highly porous structure is another advantage of utilizing the electrospinning process to create nanofiber electrode mats. The molecular mechanism of charge storage in the nanofiber mat is unclear. However, research has shown that ion size close to the pore size of the nanofiber structure provides the most efficient capacitance [17]. Also, research by Ania et al. [18] showed that some ions are being desolvated or partially desolvated in the pores of the nanofiber porous structures. Furthermore, Frackowiak et al. [19] have demonstrated a pseudo-faradaic charge transfer type behavior in the porous regions of the nanofiber structure that is believed to be caused by nitrogenated functionalities that reduce interface losses. Hence, it is believed the nanofiber mats created by the electrospinning process provide good ionic flow within its porous regions and ion desolvation within the mat's structure that contributes to increased charge storage.

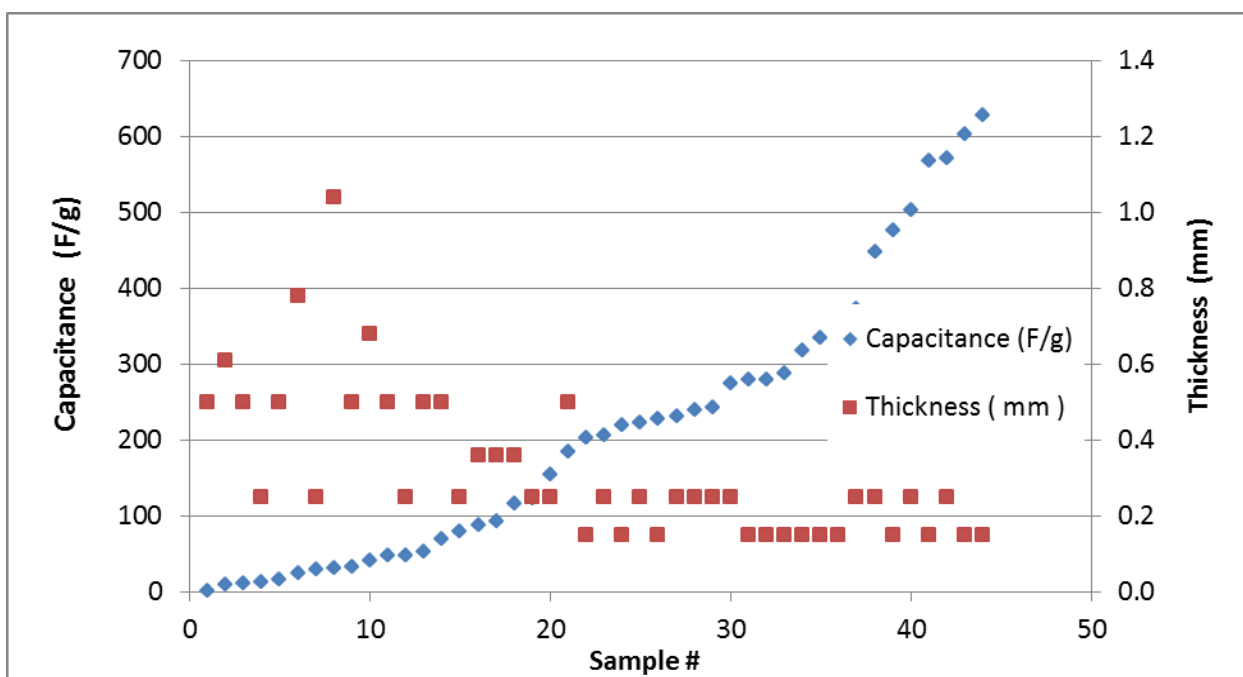


Figure 12. Nanofiber Electrode Thickness (mm) vs. Capacitance (F/g)

On the other hand, the TEM image analysis of the lower capacitance 15% graphene, 10% (CB) and 8% PAN suggests that it is mainly a turbostratic structure Figure 11. This structure is a porous intermediate stage between an amorphous carbon and a graphene sheet-type structure that is believed to have fewer vacancies than the amorphous structure and therefore, lower ion desolvation resulting in a lower energy storage capacity.

These results indicate that the initial solution carbon content plays a role in the atomic structure and energy storage Figure 7. The results clearly show the lower carbon mole content of the initial

solution resulted in the highest capacitance and the higher mole content solutions resulted in the lowest capacitance.

5. CONCLUSION

Supercapacitor cells were constructed using nanofiber electrodes fabricated via the electrospinning process to study the effects of graphene and carbon black content on electrode structure and supercapacitor performance. The supercapacitor cells constructed using a lower carbon electrospinning mixture (15% and 25% graphene with 8% PAN and the 8% PAN only concentration) resulted in the highest capacitance values ranging from 374-428 F/g on average, but with high sample to sample variation. The cells fabricated from the higher carbon solutions (15%, 25% and 35% graphene with 10% (CB) and 8% PAN concentration) showed lower capacitance values below 200 F/g, however, sample to sample variation was improved. It is concluded that the initial solution carbon content of the electrospinning mixture has a strong influence on capacitance, with the lower carbon electrospinning mixtures producing nanofiber mats with the highest capacitance. In addition, optimizing the carbon content is important to reduce sample to sample variation in capacitance and maintain high capacitance values.

Spectrum and image analysis performed on the nanofibers indicates the lower carbon mole content samples had an amorphous structure, which corresponded to the highest capacitance; while the lower capacitance value showed a turbostratic structure. No correlation was observed between nanofiber mat thickness and capacitance for the tested samples, this is attributed to the very porous structure of stacking nanofibers on top of each other; which creates high porous regions that provide a good path for ions to travel through. The molecular mechanism of charge storage in the higher capacitance value samples, in the low carbon mole solution, require further study; however, recent research is pointing to nitrogenated functionalities and ion desolvation in the amorphous structure, as possible causes for the higher capacitance values.

ACKNOWLEDGEMENTS

The authors acknowledge and appreciate the contributions and the use of equipment from the Department of Chemical Engineering, the Department of Mechanical Engineering and the Research Resource Center at the University of Illinois at Chicago, USA; and the PhD advisory committee, especially Dr. Said Al-Hallaj. This research was self-funded.

References

1. X. Mao, A. Hatton, G. Rutledge, *Current Organic Chemistry*, 17 (2013) 1390-1401.
2. W. Liu, X. Yam, J. Lang, C. Peng, Q. Xue, *J. Mater. Chem.*, 22 (2012) 17245-17253.
3. J. Keskinen, S. Tuurala, M. Sjödin, K. Kiri, L. Nyholm, T. Flyktman, M. Strømme, M. Smolander, , *Synthetic Metals*, 203 (2015) 192-199.
4. E. Garcia-Breijo, G. Prats-Boluda, R. Lidon, J. Vicente, Y. Ye-Lin, J. Garcia-Casado, *Microelectronics International*, 32 (2015) 107-103.
5. K. Kim, *J. Chemistry*, 314893 (2015) 1-7.

6. K. Nam, K. Kim, *J. Electrochem. Soc.*, 153 (2006) A81–A88.
7. X. Shi, W. Zhou, D. Ma, Q. Ma, D. Bridges, Y. Ma, A. Hu, *J. Nanomaterials*, 2015 (2015) 140716.
8. X. Mao, T. Hatton, G. Rutledge, *Current Organic Chemistry*, 17 (2013) 1390-1401.
9. K. Chan, *J. Power Sources*, 142 (2005) 382-388.
10. C. Kim, Y. Choi, W. Lee, K. Yang, *PBFC*, 50 (2004) 883-887.
11. A. Pandolfo, A. Hollenkamp, *J. Power Sources*, 157 (2006) 11-27.
12. Y. Ying, J. Zhidong, L. Qiang, L. Jianan, G. Zhicheng, *IEEE Transactions on Dielectrics and Electrical Insulation*, 16 (2009) 409-416.
13. D. Wu, Z. Xiao, L. Deng, Y. Sun, Q. Tan, L. Dong, S. Huang, R. Zhu, Y. Liu, W. Zheng, Y. Zhao, L. Wang, D. Sun, *Nanomaterials*, 135 (2016) 1-12.
14. R. Lin, P.L. Taberna, J. Chmiola, D. Guay, Y. Gogotsi, P. Simon, *J. Electrochem. Soc.*, 156 (2009) A7-A12.
15. M. Toupin, D. Belanger, I. Hill, D. Quinn, *J. Power Sources*, 140 (2005) 203-210.
16. J. Chmiola, G. Yushin, Y. Gogotsi, C. Portet, P. Simon, P.L. Taberna, *Science*, 313 (2006) 1760-1763.
17. C. Largeot, C. Portet, J. Chmiola, P.L. Taberna, Y. Gogotsi, P.J Simon, *Am. Chem. Soc.*, 130 (2008) 2730-2731.
18. C. Ania, J Pernak, F. Stefaniak, E. Raymundo-Piñero, F. B´eguin, *Carbon*, 47 (2009) 3158-3166.
19. E. Frackowiak, Q. Abbas, F. B´eguin, *Journal of Energy Chemistry*, 22 (2013) 226–240.
20. F. Ko, Y. Gogotsi, A. Ali, N. Naguib, H. Ye, G. Yang, C. Li, P. Willis, *Adv Mat*, 15 (2003) 1161-1165.
21. J. Wang, S. Kaskel, *J. Mater. Chem.*, 22 (2012) 23710.
22. Z. Yu, L. Tetard, L. Zhai, J. Thomas, *Energy Environ Sci.*, 8 (2015) 702-730.
23. H. Zhenga, J. Li, X. Songb, G. Liub, V. Battagliab, *Electrochimica Acta*, 71 (2012) 258– 265.
24. R. Zhao, J. Liu, J. Gu, *Applied Energy*, 139 (2015) 220–229.